Materials Research Proceedings **27** (2023) 111-118 https://doi.org/10.21741/9781644902455-14

Estimating the probability of detection of cracks in metal plates using lamb waves

Faeez Masurkar[1,a,*], Fangsen Cui[1,b]

[1]Institute of High-Performance Computing, A*STAR (Agency for Science, Technology, and Research) Research Entities, Singapore 138632

[a]Masurkar_Faeez_Aziz@ihpc.a-star.edu.sg, [b]cuifs@ihpc.a-star.edu.sg

Keywords: Lamb-Waves, Probability of Detection, Data-Driven Damage Estimation, PVDF Sensors, Metal Plates

Abstract. This paper focusses on the development of a data-driven damage detection method to quantify fatigue crack in metal plates using Lamb waves and its reliability using a probability of detection (POD) technique. The guided Lamb waves are generated and sensed using an array of direct-write (DW) polyvinylidene fluoride (PVDF) annular comb shaped transducers designed to explicitly generate a desired guided wave mode in the test specimen. The annular comb design helps generate a single desired wave mode in the specimen thereby suppressing the energy of other wave modes that can be generated simultaneously. The guided wave responses are obtained through a simulation study and are recorded at different progressions of crack. A damage index (DI) is constructed as a function of crack size that can effectively track the change in ultrasonic response variations and for diagnosing fatigue crack in the metallic specimens. This DI is then further used in the POD model to estimate the crack detection probability. The POD curves can be helpful to check the reliability of the proposed inspection system as well as identify the critical experimental parameters that can significantly influence the crack detection results.

Introduction

Non-Destructive testing (NDT) systems utilize scattered, permanently attached transducers at critical regions of structural failure, and employ diagnostic methods or algorithms to extract the health-related sensitive information from the captured data [1]. Ultrasound based NDT has gathered lot of attention by researchers worldwide as they can be excited and sensed by cheap sensors. However, the ultrasonic guided waves are highly dispersive and therefore a careful selection of the frequency-mode pair is vital in developing an effective NDT system. Further, the physics of guided wave propagation could be quite complicated if effective actuation and reception strategies are not adopted [2].

Forsyth et.al. [3] discussed the theoretical foundations for evaluating the effect of multiple inspections, and examine data from the experiments against this framework to demonstrate the effectiveness of POD from multiple tests. Meeker et.al [4] reviewed the basics of POD and discussed how it can be effectively applied to NDT studies by modification and extension of pre-existing methods for estimating POD. Virkkunen et.al [5] presented a comparison between â versus a and hit/miss for two entirely different data sets and found both models may yield drastically different results, if the true hit/miss output is based on an individual judgement and not on an automated signal threshold. Adam et.al [6] discussed the relationship between NDT and POD and a case study is further presented for the development of POD curves using a model-assisted formulation. Mishra et.al [7] studied the acousto-ultrasound based SHM technique quantified as "in-situ NDE" through a POD method based on a model assisted approach in the context of fatigue crack detection.

The present study focusses on the NDT of an Al 6060 specimen to evaluate the crack presence and its progression using ultrasonic guided waves. Firstly, a suitable frequency-mode pair was

identified through the dispersion diagram best suited to detect the crack. Next, a DI was constructed as a function of crack size to quantify the damage progression. Lastly, a POD curve was constructed to check the reliability of the proposed inspection system as well as the probability with which a crack of given size can be detected. Finally, findings from the present study were summarized.

Methodology

The present study focusses on the crack detection and tracking its progression using the desired ultrasonic guided wave mode generated using the 3-electrode annular comb array design of PVDF transducers. A similar array is used on the opposite side to receive the ultrasonic guided waves. Thus, the propagating ultrasonic waves can be received in pulse-echo as well as pitch catch configurations. The data is collected for intact state of the specimen and during several progressions of fatigue crack. Further, a DI is constructed through the received time domain responses to quantify the crack which is further used in the POD model to predict the probability with which each crack size can be detected. The background of the POD model is illustrated in the following sub-section.

Probability of detection model

Let 'a' be the actual crack size, '$\hat{a}$' be the calibrated crack size, and 'x' and 'y' be the natural logarithm of the actual and calibrated crack size respectively. The linear relationship between 'x' and 'y' can be represented as [8],

$$y = \beta_0 + \beta_1 x + \epsilon; \tag{1}$$

Where 'ϵ' is the error between the fitted data and actual data, and has normal distribution with mean $\mu = 0$ and 'δ^2' as its variance. The standard normal variate can be written as;

$$Z = \frac{y-(\beta_0+\beta_1 x)}{\delta}; \text{ which has a standard normal distribution as,} \tag{2}$$

$$\phi(z) = \frac{1}{\sqrt{2\pi}} e^{\frac{-Z^2}{2}} \tag{3}$$

The cumulative distribution function (CDF) of a standard normal distribution is;

$$Q(z) = \int_z^{\infty} \phi\,(Z)\, dz \tag{4}$$

Thus, the POD of any given crack size can be obtained as follows,

$$\text{POD}\,(x) = \text{POD}\,(y > y_{th}) = Q\left[\frac{y_{th}-(\beta_0+\beta_1 x)}{\delta}\right] \tag{5}$$

Where, y_{th} is the lowest size of crack that can be detected. The complement of the Standard CDF is,

$$Q[-Z] = 1 - Q[Z] \tag{6}$$

$$\text{POD}\,(a) = \text{POD}\,(y > y_{th}) = 1\text{-}\, Q\left[\frac{x - \left(\frac{y_{th}-\beta_0}{\beta_1}\right)}{\frac{\delta}{\beta_1}}\right] = 1\text{-}\, Q\left[\frac{\log_e(a) - \left(\frac{y_{th}-\beta_0}{\beta_1}\right)}{\frac{\delta}{\beta_1}}\right] \tag{7}$$

Thus, mean = $\left(\frac{y_{th}-\beta_0}{\beta_1}\right)$ and standard deviation = $\frac{\delta}{\beta_1}$. These can be further used to estimate the POD curve as a function of actual crack size.

Numerical study

In the present study, the ultrasonic guided waves are obtained using a 2D Finite element (FE) set up. For this purpose, 3-electrode annular comb array design of PVDF transducers is modeled and

time-domain data is collected in pulse echo and pitch catch configurations. The materials used in the simulation and their mechanical properties are presented in the following subsection.

Material description and defects

The specimen used for the present study is a 2.286 mm thick Aluminum plate with notch of different sizes to simulate crack progression as shown schematically in Fig.1. The crack size is increased as a function of the percentage of plate thickness. The overall dimensions of the plate specimen and the sensors are shown in Fig.1.

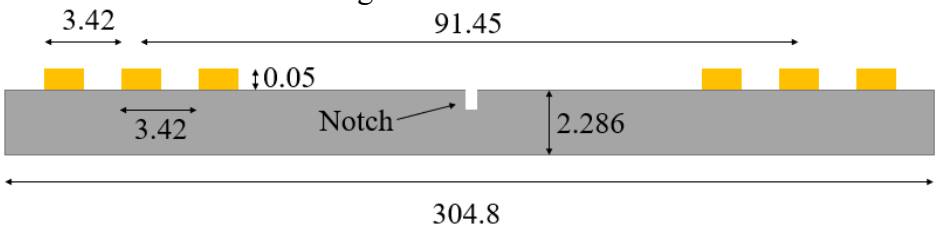

Fig.1 Schematic of the specimen model (Note: All dimensions are in mm and figure not to scale)

Table 1 *Mechanical properties of Al 6060 material*

Material	**Thickness (mm)**	**ρ(Kg/m^3)**	**E(GPa)**	**ν [-]**	**V_L (m/s)**	**V_T (m/s)**
Al6060	2.286	2700	70	0.33	6197.82	3122

Dispersion curves & wave structures of the Al6060 specimen:

The propagation of different wave modes in the considered Al6060 specimen at different frequencies can be obtained using the dispersion curves. Therefore, dispersion curves are firstly obtained for a 2.286 mm thick Al plate and are shown in Fig.2. It can be seen that the S_1 Lamb mode at 1.75 MHz excitation frequency is a good choice from the design perspective of the PVDF sensor as well as the wave-structures of this mode show good sensitivity to the surface and embedded damages except the midplane of the specimen. The excitation applied to the PVDF sensors is a 10.5 cycles gaussian modulated sine wave signal that is centered at 1.75 MHz frequency. This time-domain excitation signal and its frequency spectrum is shown in Fig.3.

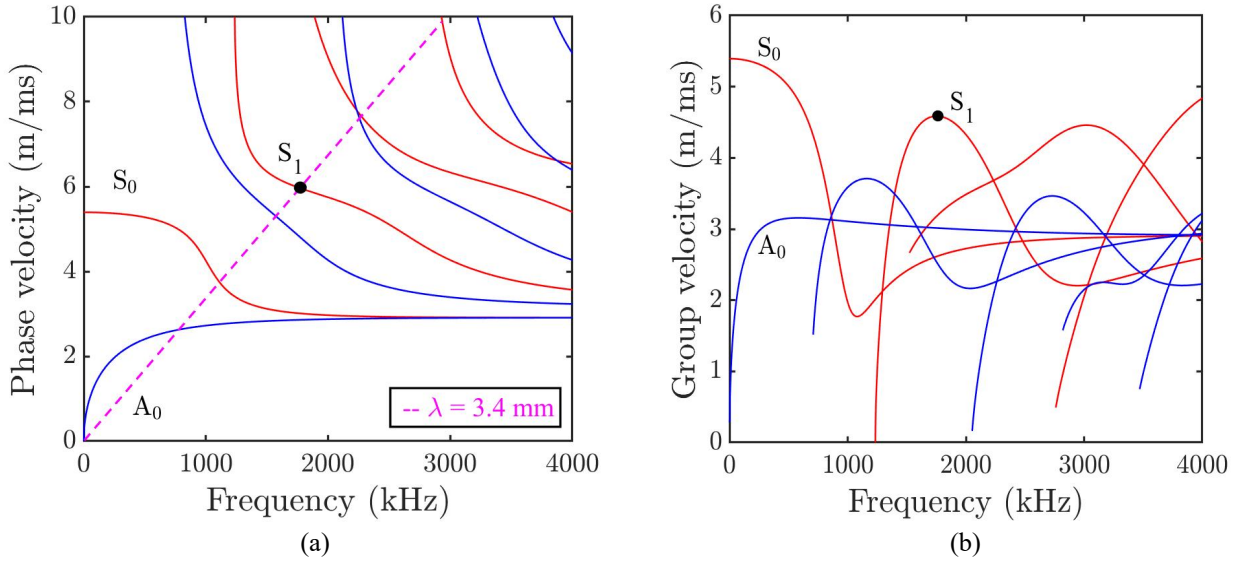

(a) (b)

Materials Research Proceedings **27** (2023) 111-118 https://doi.org/10.21741/9781644902455-14

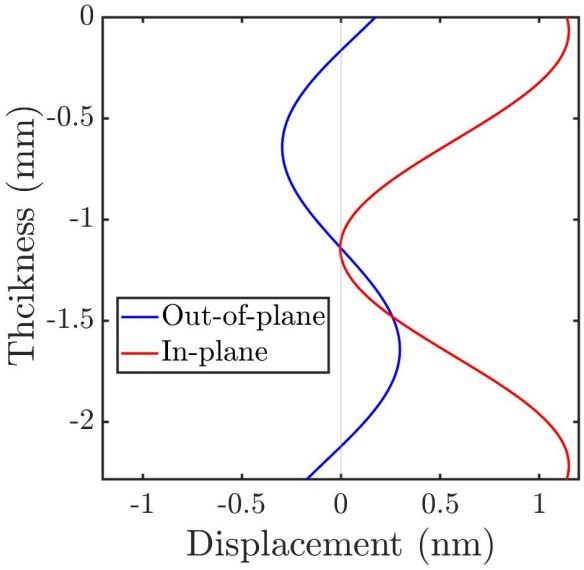

(c)

Fig.2 Dispersion Curves of the Al specimen (a) Phase velocity (b) Group velocity (c) Wave structures

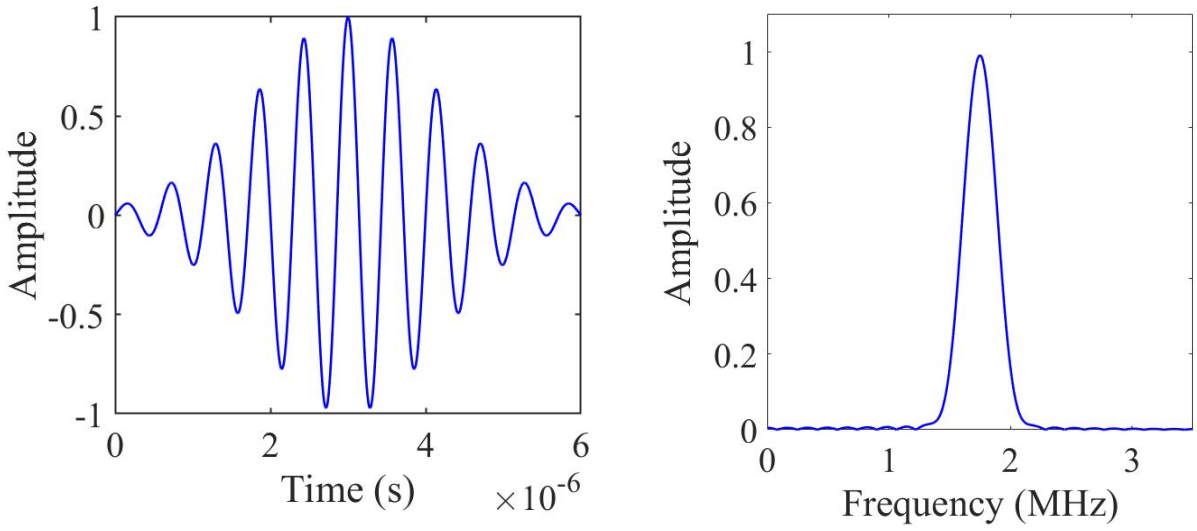

(a) (b)

Fig.3 The Excitation signal used in FE simulations (a) Time domain (b) Frequency domain

Finite Element model

In the present study, the guided wave responses were excited and sensed using a array of PVDF sensors with a spacing between each element as one-wavelengh and is shown schematically in Fig. 1. The spacing between each element is calculated from the Phase velocity dispersion curve (Fig.2(a)). In order to excite a dominant S_1 Lamb mode at 1.75 MHz excitation frequency, the wavelength should be 3.42 mm. However, it should be noted that, the excitation line with wavelength 3.42 mm also shows possible generation of other Lamb modes but those modes should be excited with lesser energy at this frequency. On the receiver side, in-plane and out-of-plane time domain responses are recorded on the sensor surface for different percents of notch depths with respect to plate thickness. Further absorbing boundary conditions are enforced at the start and end of the plate across its thickness direction. The results are discussed in the following section.

Materials Research Proceedings **27** (2023) 111-118 https://doi.org/10.21741/9781644902455-14

Results and discussions

The results of FE simulations conducted at 1.75 MHz for an intact Al specimen is presented firstly in this section. The wave propagation for an intact specimen is shown in Fig.4. It can be seen that the PVDF sensors spaced at 1.71 mm excite a dominant S_1 Lamb mode. Further, time-domain waveforms at the intact condition of the specimen recorded in a pulse echo configuration are shown in Fig.5 for the in-plane and out-of-plane motion. It shows a pure generation of S_1 Lamb mode with no potential reflections from damage.

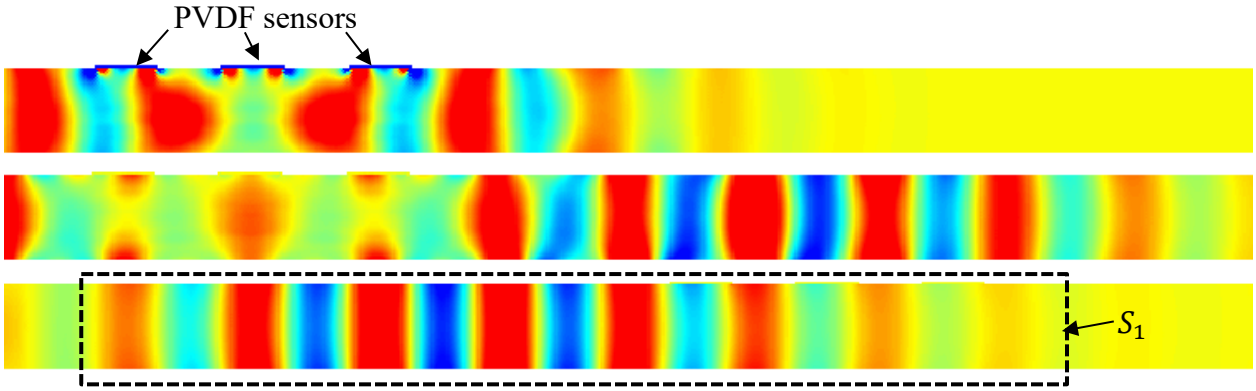

Fig.4 Wave propagation at different time instants in a intact Al specimen

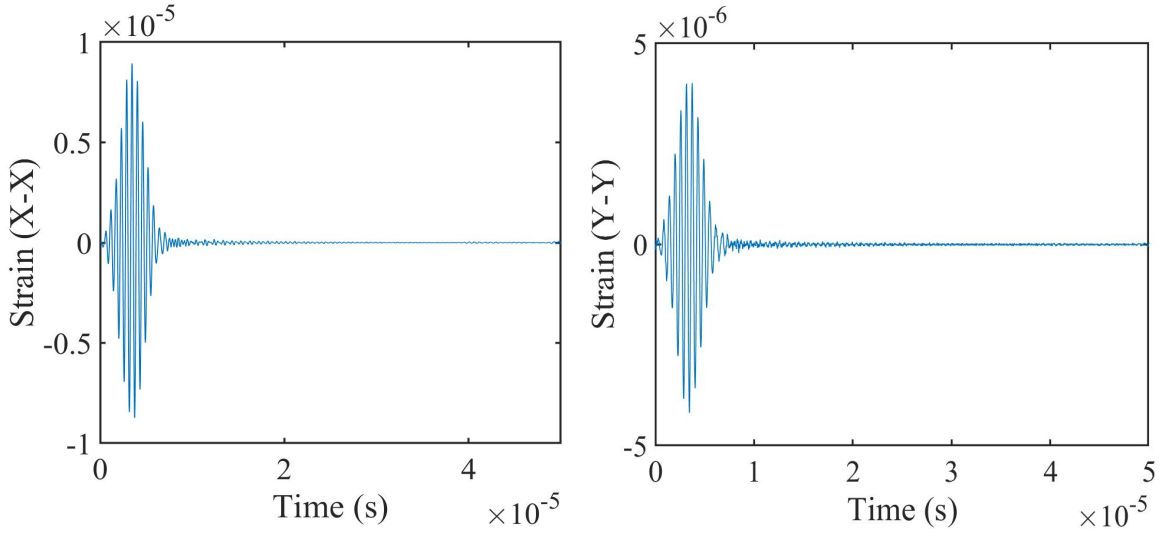

(a) In-plane (b) Out-of-plane

Fig.5 Time domain waveforms for a healthy Al specimen received at exciter (pulse echo)

The time-domain signals recorded at intact state in the pitch-catch configuration for in-plane and out-of-plane motion are shown in Figs.6(a) & 6(b) respectively. It can be seen that for a pitch-catch configuration, multiple wave modes are generated. To understand which modes are generated, a short time Fourier transformation (STFT) of both in-plane and out-of-time time domain signals is conducted and theoretical dispersion curves are overlapped on top of it. The results are shown in Figs.7(a) & 7(b) respectively. It shows that S_1 wave is dominantly generated with relatively slower velocity modes S_0 and S_2 being generated simultaneously and with lesser energy at 1.75 MHz excitation frequency.

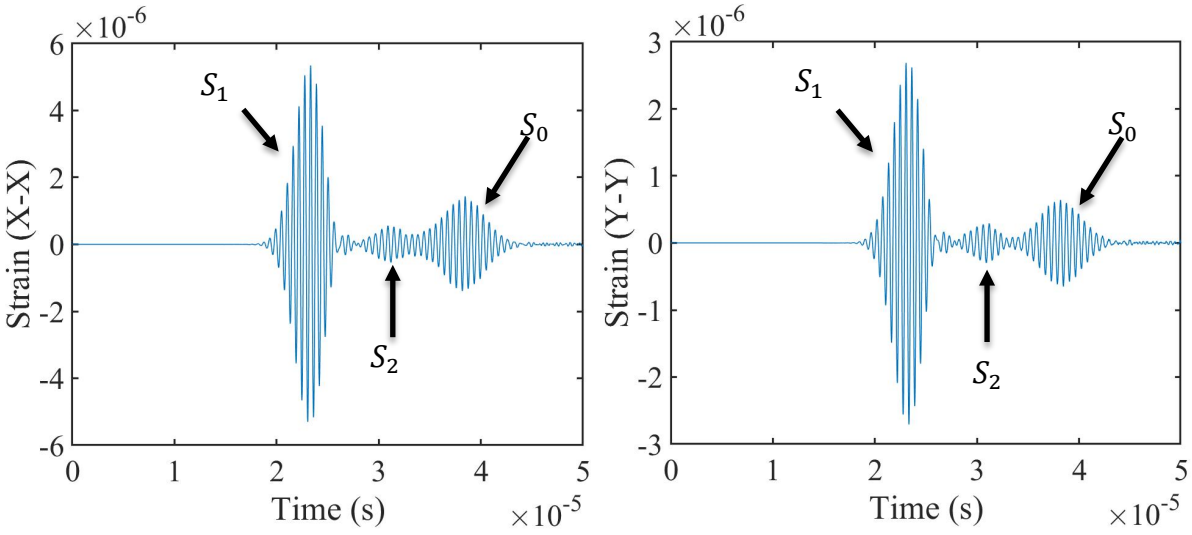

(a) In-plane (b) Out-of-plane

Fig.6 Time domain waveforms for an intact Al specimen (pitch catch)

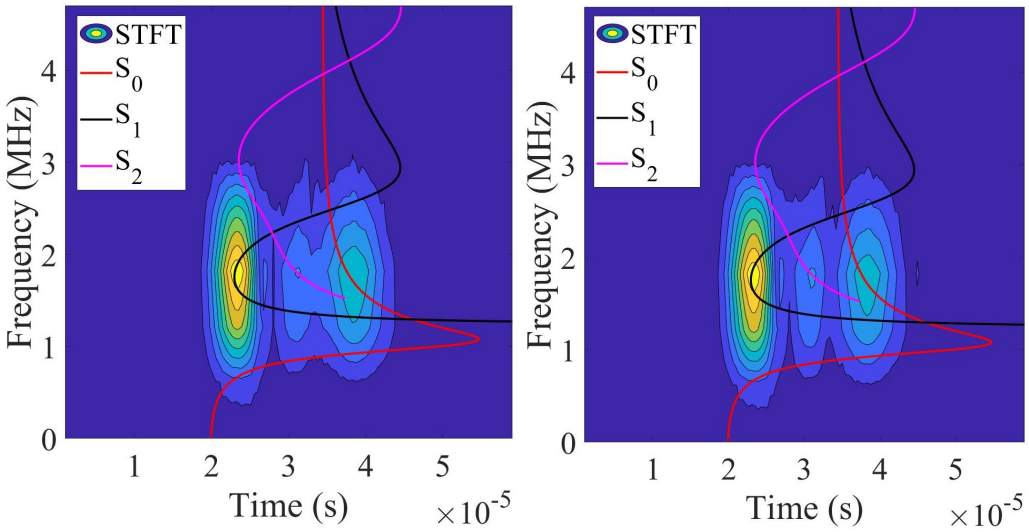

(a) In-plane (b) Out-of-plane

Fig.7 STFT of Time domain waveforms for an intact Al specimen (pitch catch)

The FE simulations are further conducted with increasing notch size in the Al specimen and time-domain signals recorded in the pulse echo and pitch-catch configuration for in-plane and out-of-plane motion. The time domain signals for pulse echo configuration in presence of damage (10% and 20% of plate thickness) are shown in Fig.8. It can be seen that for a damaged specimen, wave reflections take place from the damage and are captured in the pulse echo configuration. For brevity, only the results of intact state and damaged state where damage severity is 10% and 20% of plate thickness is presented for demonstration purposes. Thus, an index needs to be defined that can quantify the difference between the intact and damage state time domain signals. The damage index (DI) used in the present work is shown in Eq.8 as follows,

$$DI = \frac{\sum_{n=1}^{N}[E_{Current}(n) - E_{Baseline}(n)]^2}{\sum_{n=1}^{N}[E_{Baseline}(n)]^2} \quad (8)$$

Materials Research Proceedings **27** (2023) 111-118 https://doi.org/10.21741/9781644902455-14

Where $E_{Current}$ is the time domain signal at the current state of the specimen and $E_{Baseline}$ is the time domain signal at the intact state of the specimen, and n are the number of samples. The DI is then evaluated using the in-plane time domain responses recorded at intact and damaged states for different severity through Eq.8. and is presented in Fig.9(a) that shows the damage severity (normalized) as a function of growing crack size.

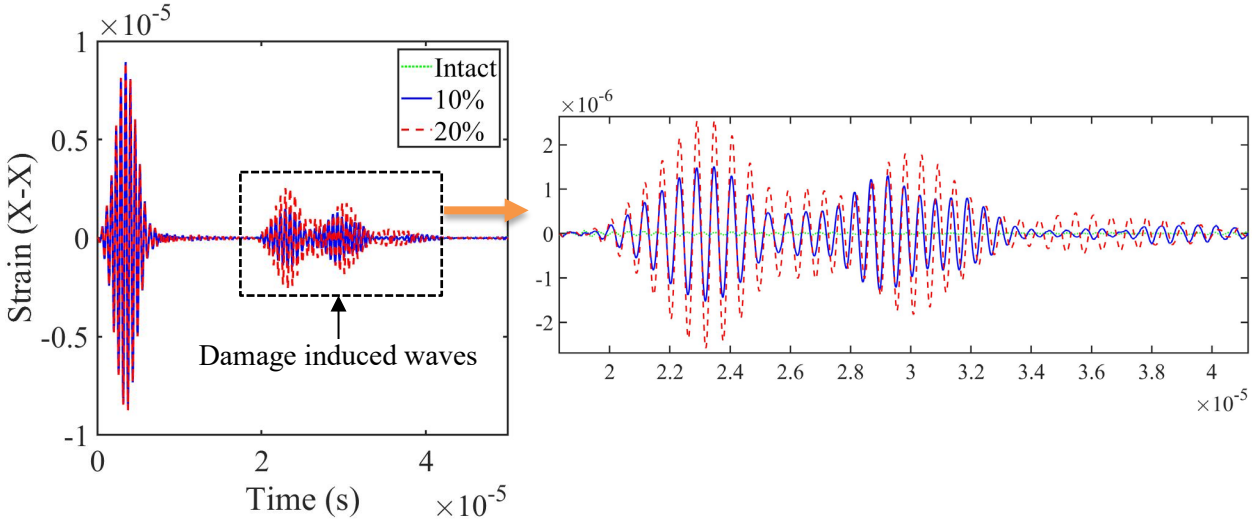

(a) (b)

Fig.8 Time domain waveforms for an Al specimen with growing crack

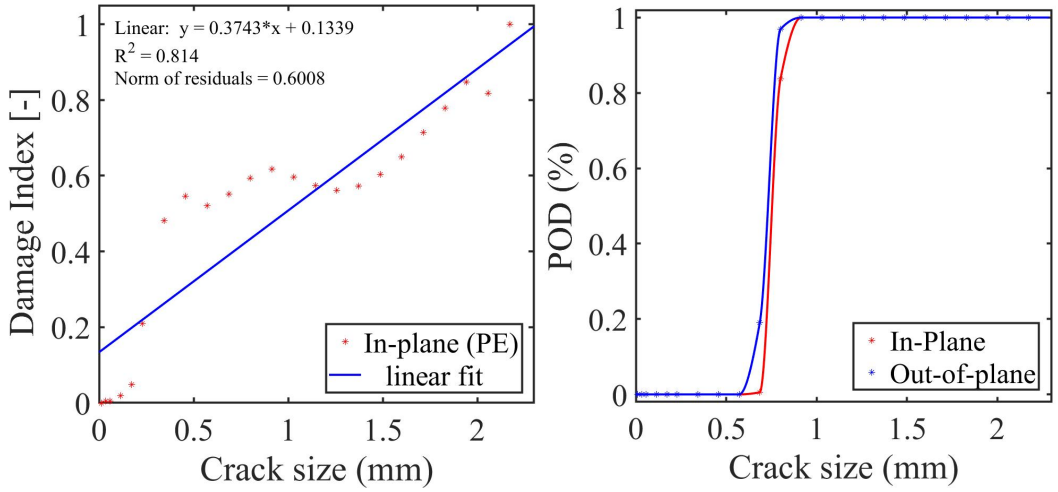

(a) Linear fit to data (b) POD

Fig.9 POD with increasing crack size at 152.4 mm in wave propagation direction from origin

It can be seen that around the mid plane a temporarily decrease in the DI is observed which is basically because of the wave structure of the S_1 Lamb mode as shown in Fig. 2(c) that is relatively in-sensitive around the midplane of the plate. Ideally, a stable increase in the DI should be achieved. However, this majorly depends on the wave mode used for inspection. Next, a linear fit is applied to the calculated DI's which yields the parameters in Eq.1, as well as the variance of the residual data set. Finally, using Eq.7, the POD curve is constructed for the in-plane and out-of-plane time domain data responses. The discrepancy between the POD curves constructed for the in-plane and out-of-plane time domain data is mainly because of the difference in the sensitivity

of the wave structures of S_1 Lamb mode for in-plane and out-of-plane motion. Overall, the crack size quantification probability is relatively same.

Summary

This paper presents the development of a damage quantification and reliability estimation technique in an Al plate specimen using Lamb waves excited through an array of annular comb shaped sensors and POD. Dispersion curves of the Al plate specimen were firstly obtained to identify the most suitable frequency-mode pair for inspection from a practical perspective. Based on the dispersion and wave structure analysis, S_1 Lamb mode at 1.75 MHz was found suitable to inspect the growing crack in the Al specimen. Time domain responses were recorded at the intact and damage states of the Al specimen in pulse echo and pitch catch configurations which were finally analyzed using a DI and POD to quantify the crack and estimate reliability. Following are the concluding remarks from the present study:

1. The employed S_1 Lamb mode was able to detect the growing crack in the Al specimen.
2. The DI constructed based on the recorded data could be helpful to quantify the crack size.
3. The POD curves can be helpful to determine the reliability of the proposed inspection method.

Acknowledgement

This work is supported by the Agency for Science, Technology and Research (A*STAR), Singapore, under the RIE2020 AME Industry Alignment Fund - Prepositioning Programme (IAF-PP) (Grant number: A19C9a0044, A20F5a0043).

References

[1] V. Janapati, F. Kopsaftopoulos, F Li, SJ Lee, FK Chang, Damage detection sensitivity characterization of acousto-ultrasound-based structural health monitoring techniques, Structural Health Monitoring. 15 (2016) 143-61. https://doi.org/10.1177/1475921715627490

[2] FA. Masurkar, NP. Yelve, Optimizing location of damage within an enclosed area defined by an algorithm based on the Lamb wave response data, Applied Acoustics. 120 (2017) 98-110. https://doi.org/10.1016/j.apacoust.2017.01.014

[3] DS. Forsyth, Structural health monitoring and probability of detection estimation, AIP Conference Proceedings. 1706 (2016). https://doi.org/10.1063/1.4940648

[4] WQ. Meeker, D. Roach, SS. Kessler, Statistical methods for probability of detection in structural health monitoring, International workshop on Structural Health Monitoring (2019). https://doi.org/10.12783/shm2019/32095

[5] I. Virkkunen, T. Koskinen, S. Papula, T. Sarikka, H. Hänninen, Comparison of â versus a and hit/miss POD estimation methods: A European viewpoint, Journal of Nondestructive Evaluation. 38(2019). https://doi.org/10.1007/s10921-019-0628-z

[6] C. Adam, J. Fisher, JE. Michaels, Model-assisted probability of detection for ultrasonic structural health monitoring, Proceedings of the 4th European-American workshop on Reliability of NDE, Berlin, Germany. (2009) 24-26.

[7] S. Mishra, SK. Yadav, FK. Chang, Reliability of probability of detection of fatigue cracks for built-in acousto-ultrasound technique as in-situ NDE, Structural Health Monitoring (2019). https://doi.org/10.12783/shm2019/32506

[8] C. Annis, E. Bray, H. Hardy, PM. Hoppe, Nondestructive evaluation system reliability assessment, United States Department of Defense, Handbook MIL-HDBK-1823A (2009).